

ACTIVE MEDIA

PACS numbers: 42.55.Ks; 82.30.Fi; 33.20.Tp
DOI: 10.1070/QE2010v040n09ABEH014357

Nonequilibrium population of the first vibrational level of $O_2(^1\Sigma)$ molecules in $O_2-O_2(^1\Delta)-H_2O$ gas flow at the output of chemical singlet-oxygen generator

M.V. Zagidullin

Abstract. **The concentrations of electron-excited particles have been determined by measuring the absolute spectral irradiance in the range of 600–800 nm of $O_2-O_2(^1\Delta)-H_2O$ gas mixture at the output of a chemical singlet-oxygen generator (SOG). A nonequilibrium population of the first vibrational level of $O_2(^1\Sigma)$ molecules has been clearly observed and found to depend on the water vapour content. In correspondence with the results of these measurements and according to the analysis of kinetics processes in the $O_2-O_2(^1\Delta)-H_2O$ mixture, the maximum number of vibrational quanta generated in the $O_2(^1\Delta) + O_2(^1\Delta) \rightarrow O_2(^1\Sigma) + O_2(^3\Sigma)$ reaction is 0.05 ± 0.03. It is concluded that the vibrational population of $O_2(^1\Delta)$ at the output of the SOG used in a chemical oxygen–iodine laser is close to thermal equilibrium value.**

Keywords: *singlet oxygen, vibrational excitation, oxygen–iodine laser.*

1. Introduction

The exchange in vibrational energy and its relaxation in O_2-H_2O gas mixture is of interest for physics of atmosphere [1, 2]; these processes have also been investigated in post-discharge oxygen flow [3]. The $O_2-O_2(a^1\Delta)-H_2O$ mixture serves as an energy source in a chemical oxygen–iodine laser (COIL). Despite significant progress in the development of high-power COILs, the mechanism of dissociation of the molecular iodine mixed with an $O_2-O_2(a)-H_2O$ flow is still to be understood. In some kinetic models the energy transfer from vibrationally excited $O_2(a)$ molecules to iodine is assumed to be the primary stage of their dissociation [4]. In this context, it is interesting to know to what extent the populations of levels of vibrationally excited oxygen molecules in $O_2-O_2(a)-H_2O$ gas mixture exceed their thermal equilibrium populations. This excess of the population of vibrational levels of oxygen molecules above the thermal value is obviously determined by the ratio of the pump and relaxation rates of vibrational levels of these molecules. In a chemical singlet-oxygen generator (SOG) $O_2(a)$ molecules are produced in the reaction of gaseous chlorine with an alkaline solution of hydrogen peroxide [5]. In the $O_2-O_2(a)-H_2O$ mixture, emerging from the peroxide alkaline solution, oxygen molecules in the second electron-excited state $b^1\Sigma$ are formed in the reaction

$$O_2(a) + O_2(a) \rightarrow O_2(b) + O_2(X) \quad (1)$$

which is followed by the quenching reaction

$$O_2(b) + H_2O \rightarrow O_2(a) \text{ (or } O_2(X)) + H_2O. \quad (2)$$

Reactions (1) and (2) can be primary sources of vibrationally excited O_2 and H_2O molecules [6–8]. Fast VV [9] and EE exchanges [1] between oxygen molecules lead to the formation of a vibrational reservoir, which contains oxygen molecules in the X, a, and b states. Water molecules are captured by this reservoir through the fast resonant VV exchange with oxygen molecules [10]. However, VR and VT relaxations, as well as the deexcitation on walls lead to energy loss from this reservoir. It was previously established that the probability of forming $O_2(b, v = 2)$ in reaction (1) is 0.64, whereas the probability of forming $O_2(b, v = 1)$ does not exceed 0.04 [3]. In the earlier publication [6] the probability of $O_2(b, v = 1)$ production in reaction (1) was found to be 0.05, but no $O_2(b, v = 2)$ molecules were found. As far as we know, there are no other data in the literature on quantitative determination of the yield of vibrationally excited oxygen molecules in reactions (1) and (2).

The purpose of this study was to determine the excess content of vibrationally excited $O_2(b)$ and $O_2(a)$ molecules above their thermal equilibrium content, depending on the amount of water vapour in the $O_2-O_2(a)-H_2O$ gas mixture generated by a SOG and estimate the maximum number of vibrational quanta formed in oxygen molecules as a result of reaction (1).

2. Experimental

A schematic of the experimental setup is shown in Fig. 1. An $O_2-O_2(a)-H_2O$ gas mixture was formed by a jet SOG [11], which worked at a temperature of hydrogen peroxide alkaline

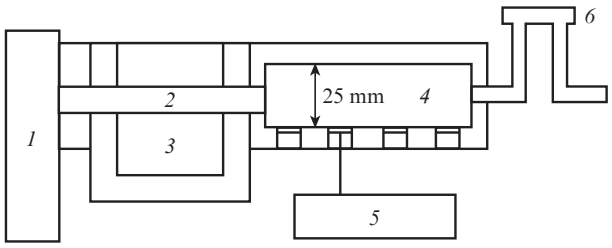

Figure 1. Schematic of the experimental setup: (*1*) SOG, (*2*) WVT, (*3*) bath with coolant, (*4*) ORDERS, (*5*) AvaSpec-3648 spectrometer, and (*6*) optical cell.

M.V. Zagidullin Samara Branch of P.N. Lebedev Physics Institute, Russian Academy of Sciences, Novo-Sadovaya ul. 221, 443011 Samara, Russia; e-mail: marsel@fian.smr.ru

Received 12 May 2010; revision received 25 June 2010
Kvantovaya Elektronika **40** (9) 794–799 (2010)
Translated by Yu.P. Sin'kov

solution of –13 °C and a chlorine molar flow rates of 0.4 mmol s^{-1}, and transmitted through a water vapour trap (WVT). The trap is followed by an optical diagnostic system (ODS) – a caprolon channel having a rectangular cross section and the following sizes: length 8 cm, width L = 2.5 cm, and height 0.8 or 1.5 cm, with several holes closed by optical windows 2 mm thick. The experiments were performed at a total pressure of 26 Torr in the SOG and ODS. The absolute spectral irradiance of the O_2–$O_2(a)$–H_2O mixture in the range of 600–800 nm was measured with an AvaSpec-3648 optical fibre spectrometer (Avantes, Netherlands) with a CCD detector line. The absolute spectral sensitivity R of the spectrometer (in photons $counts^{-1}$ cm^{-2} nm^{-1}) was calibrated by the manufacturer with an error of 9.5%. By definition, the $R(\lambda)\delta\lambda$ value is the number of photons emitted from 1 cm^2 of the surface of diffuse continuous-spectrum source into a narrow spectral range $\lambda,\lambda+\delta\lambda$, corresponding to one pixel of the CCD line, which leads (at the detecting fibre axis oriented normally to the emitting surface) to an increase in the number of its counts by unity. The receiving end of the optical fibre was located directly before the optical window. The spectrometer recorded the radiation from only the bulk of the gas present in a cone with an angle of 15° and the vertex located in the fibre core, or only from the central part of the gas flow: a layer with a height $\delta h \approx 2$ mm between the ODS walls. Simultaneously we recorded collision-induced emission spectra: $O_2(a,v=0) + O_2(a,v=0) \rightarrow O_2(X,v=0) + O_2(X,v=0) + h\nu$ ((0,0–0,0) band, λ = 634 nm); $O_2(a,v=0) + O_2(a,v=0) \rightarrow O_2(X,v=1) + O_2(X,v=0) + h\nu$ ((0,0–0,1) band, λ = 703 nm); and (0–0), (1–1), (1–0), and (2–2) bands of the b → X system. The number of counts of the CCD line $C(\lambda)$ was used to determine the specific volume spectral irradiance $S_{exp}(\lambda) = 4C(\lambda)R(\lambda)/(t_e L T_\lambda)$ of the gas in the ODS. Here, $T_\lambda \approx 0.92$ is the optical-window transmittance in the range λ = 600–800 nm and t_e is the exposure time. The absolute concentrations n_a and n_b of $O_2(a,v=0)$ and $O_2(b,v=0)$ molecules were found from the relations

$$k_d n_a^2 = \int S_{exp}(\lambda)\mathrm{d}\lambda, \quad A_b n_b = \int S_{exp}(\lambda)\mathrm{d}\lambda, \tag{3}$$

where $k_d = (6.06 \pm 0.19)\times10^{-23}$ cm^3 s^{-1} is the collision-induced emission rate [(0,0–0,0) band] and $A_b = (7.48 \pm 0.08)\times10^{-2}$ s^{-1} is the Einstein coefficient of the b–X(0–0) transition. The integration in the right-hand side of (3) was performed over the corresponding spectral bands. The k_d value was determined from the relation

$$k_d = \frac{g_{low}}{g_{up}}\frac{8\pi c}{\lambda^2}B_d,$$

where $B_d = (3.23 \pm 0.1)\times10^{-43}$ cm^4 is the integrated cross section of collision-induced absorption $O_2(X,v=0) + O_2(X,v=0) + h\nu \rightarrow O_2(a,v=0) + O_2(a,v=0)$ [12]; $g_{low}/g_{up} = 1$ is the ratio of statistical weights of the states of $O_2(a):O_2(a)$ and $O_2(X):O_2(X)$ dimoles, involved in the radiative process [13]; and λ = 634 nm is the central wavelength of the collision-induced absorption band. The Einstein coefficient A_b was calculated using the latest data for the b–X(0–0) band strength [14].

The water vapour content in the ODS is estimated using the condition for the balance of production (1) and destruction (2) rates of $O_2(b)$ molecules: $k_1 n_a^2 \approx k_2 n_w n_b$; hence,

$$n_W \approx \frac{k_1}{k_2}\frac{n_a^2}{n_b}, \tag{4}$$

where n_w is the water concentration; $k_1 = (2.7 \pm 0.4)\times10^{-17}$ cm^3 s^{-1} and $k_2 = (6.7 \pm 0.53)\times10^{-12}$ cm^3 s^{-1} are the rate constant of reactions (1) [15] and (2) [16], respectively. As will be shown below, formula (4) fairly exactly determines the water concentration, because in the experiments the destruction rate of $O_2(b)$ molecules in reaction (2) significantly exceeds their destruction rate upon collisions with O_2 and Cl_2 molecules and on ODS walls. When calculating n_w, we assumed that the ratio k_1/k_2 is temperature-independent in the range of 300–400 K. The error in determining n_w from formula (4) was estimated to be about 30% (because of the uncertainty in the k_1, k_2, and R values).

To estimate the gas temperature and $O_2(b,v=1)$ content, we compared the experimental and synthesised emission spectra of the b–X transition in O_2 molecules. The partially resolved rotational structure of the b–X(0–0) band was synthesised using the HITRAN database [17] and the instrumental function of the spectrometer at a wavelength of 762 nm. The total synthesised spectrum of the b–X(0–0) and b–X(1–1) bands can be presented as

$$S(\lambda, T) = S_{00}(\lambda, T) + S_{11}(\lambda, T), \tag{5}$$

where $S_{00}(\lambda, T)$ and $S_{11}(\lambda, T) = 0.85 f_{b1} S_{00}(\lambda - \Delta\lambda, T)$ are the synthesised spectra of the (0–0) and (1–1) bands at a rotational temperature T; $f_{b1} = n_{b1}/n_b$ is the $O_2(b,v=1)$ fraction; n_{b1} is the $O_2(b,v=1)$ concentration; 0.85 is the ratio of Franck–Condon factors [18] of the (1–1) and (0–0) transitions of the b–X system; and $\Delta\lambda$ = 8.91 nm is the spectral shift of the (0–0) and (1–1) bands. Both $S_{exp}(\lambda)$ and $S(\lambda, T)$ were normalised to unity in the spectral peak of the R branch of the (0–0) band. $S(\lambda, T)$ was fitted to $S_{exp}(\lambda)$ in the wavelength range of 763–780 nm to determine T and f_{b1}. The total content f_{b1} was represented as the sum of two components: $f_{b1} = f_{b1k} + f_{b1T}$, where $f_{b1T} = \exp(-2021/T)$ is the thermal equilibrium content of $O_2(b,v=1)$ molecules and f_{b1k} is its nonequilibrium fraction.

The chlorine concentration was determined (with an error of 2×10^{15} cm^{-3}) from the absorption of nitrogen laser radiation in the optical cell located below the ODS (along the flow direction), where the gas temperature was equal to that of walls (295 K). The pressures in the SOG, ODS, and optical cell were measured with an error of 1.5%. The known values of pressure, temperature, and concentrations n_w, n_a, and n_b in the ODS were used to calculate the chlorine concentration (n_{Cl_2}) and the total concentration oxygen (n_{O_2}), the water content ($F_w = n_w/n_{O_2}$), the $O_2(a)$ yield ($Y = n_a/n_{O_2}$), and the degree of chlorine utilisation ($U_{Cl_2} = n_{O_2}/(n_{Cl_2} + n_{O_2})$).

3. Results

One of the $C(\lambda)$ spectra recorded for the exposure time t_e = 4 s is shown as an example in Fig. 2. These spectra were measured at a WVT temperature of –80 °C for an ODS 0.8 cm high, through an optical window located 4 cm below (along the flow) the WVT output. No emission in the (2–2) (λ = 780 nm) and (2–1) (λ = 695 nm) bands of the b–X transition was revealed. The presence of $O_2(b,v=1)$ molecules in the gas flow is evidenced by the (1–0) emission band (Fig. 2, inset) against the background of the collision-induced (0,0–1,0) band. The normalised $S_{exp}(\lambda)$ and $S_{00}(\lambda, 370\ K)$ spectra of the b–X system in the range of 763–778 nm are presented in Fig. 3. First,

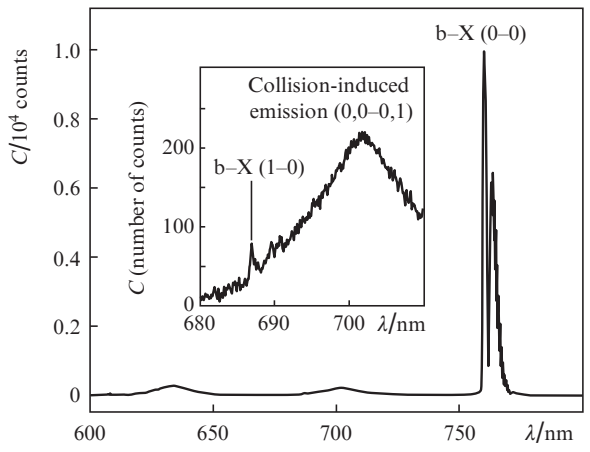

Figure 2. Emission spectrum of singlet oxygen in the range of 600–800 nm. The inset shows the emission spectrum in the range of 680–710 nm, magnified by a factor of 20.

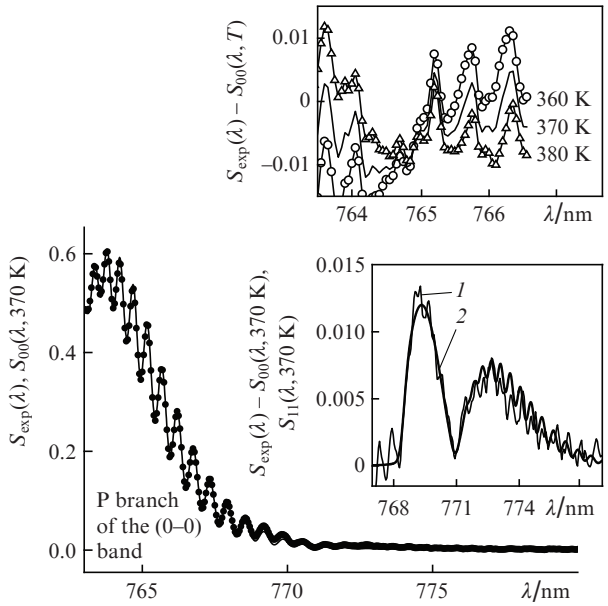

Figure 3. Normalised experimental $S_{exp}(\lambda)$ (•) spectrum $S_{00}(\lambda, 370\ K)$ and synthesised spectrum (solid line) of O_2(b) emission in the range of 763–778 nm. The insets show (top) the difference $S_{exp}(\lambda) - S_{00}(\lambda, T)$ in the peak of the P branch of the b–X(0–0) band at three temperatures and (bottom) the difference $S_{exp}(\lambda) - S_{00}(\lambda, 370\ K)$ (*1*) and synthesised $S_{11}(\lambda, 370\ K)$ spectrum (*2*) at $f_{b1} = 0.014$.

the synthesised $S_{00}(\lambda, T)$ spectrum was fitted to $S_{exp}(\lambda)$ near the peak of the P branch of the b–X(0–0) band. Figure 3 (top inset) shows the difference $S_{exp} - S_{00}(\lambda, T)$ in the range of 763.5–766.5 nm for three temperatures T to illustrate the fitting procedure. Since the minimum of $|S_{exp} - S_{00}(\lambda, T)|$ is obtained at T = 370 K and the differences $|S_{00}(\lambda, 370\ K) - S_{00}(\lambda, 380\ K)|$ and $|S_{00}(\lambda, 370\ K) - S_{00}(\lambda, 360\ K)|$ exceed the relative noise level of the CCD line (10^{-3}), the gas temperature is 370 K with an error not larger than 10 K. The difference $S_{exp}(\lambda) - S_{00}(\lambda, 370\ K)$ in the wavelength range of 767–778 nm is shown in Fig. 3 (bottom inset). The minimum discrepancy between $S_{11}(\lambda, 370\ K)$ and $S_{exp}(\lambda) - S_{00}(\lambda, 370\ K)$ in Eqn (5) is obtained at $f_{b1} \approx 1.4\times10^{-2}$. Thus, in this specific test the thermal part of the content of vibrationally excited $O_2(b, v=1)$ is $f_{b1T} = (4.2 \pm 1)\times10^{-3}$ and the nonequilibrium part is $f_{b1k} = f_{b1} - f_{b1T} \approx (1 \pm 0.1)\times10^{-2}$. The error of $\pm10^{-3}$ in determining f_{b1k} is due to the uncertainty in the gas temperature (±10 K) and the CCD line noise (±5 counts). In this specific experiment we obtained the following concentration components: $n_{O_2} = 6.6\times10^{17}$ cm^{-3}, $n_a = 2.3\times10^{17}$ cm^{-3} ($Y \approx 34\%$), $n_b = 8.5\times10^{14}$ cm^{-3}, $n_{Cl_2} = 2.8\times10^{16}$ cm^{-3} ($U_{Cl_2} \approx 94\%$), and $n_w = 2\times10^{14}$ cm^{-3} ($F_w \approx 3\times10^{-4}$). The error in determining n_w and F_w from (4) in this test can be estimated as follows. At the maximum (from the known values) probability of O_2(b) destruction on nonmetallic surfaces, $\sim10^{-2}$ [6], an estimation of the O_2(b) destruction rate on walls yields ~60 s^{-1} [15]. The total O_2(b) destruction rate under interaction with O_2(X) and Cl_2 molecules is estimated to be 40 s^{-1} at the corresponding quenching-rate constants of 4×10^{-17} cm^3 s^{-1} [19] and 4.5×10^{-16} cm^3 s^{-1} [20], respectively. The O_2(b) destruction rate in reaction (2) is 1.3×10^3 s^{-1}. Thus, the systematic error in determining n_w from (4) does not exceed 8%.

In a series of experiments the water vapour concentration in the O_2(X)–O_2(a)–H_2O flow was varied by changing the temperatures of peroxide alkaline solution and coolant in the WVT. Depending on the WVT temperature and gas-dynamic conditions, the degree of chlorine utilisation was 90%–98% and the singlet oxygen yield was 32%–38% at a distance of 4 cm from the WVT. The gas temperature changed within 340–390 K by varying the O_2(a) concentration in the range of $(2.1–2.5)\times10^{17}$ cm^{-3}. The dependence of f_{b1k} on the water vapour content F_w, obtained in a series of experiments, is shown in Fig. 4. It can be seen that the nonequilibrium fraction $f_{b1k} \approx 10^{-2}$ barely changes at $F_w < 10^{-3}$. The error in determining F_w can only shift the upper boundary of this range. Therefore, in this range of F_w values water molecules are not the main relaxant for vibrationally excited oxygen molecules. Random changes in the degree of chlorine utilisation within 90% – 98% from test to test did not affect the f_{b1k} value. Beginning with 10^{-3}, an increase in F_w leads to a decrease in the f_{b1k} content, which is indicative of the increasing role of water molecules in the relaxation of vibrational energy. At $F_w \geq 10^{-2}$ the $f_{b1k} \approx 0$ value is approximately zero within an error of 10^{-3}.

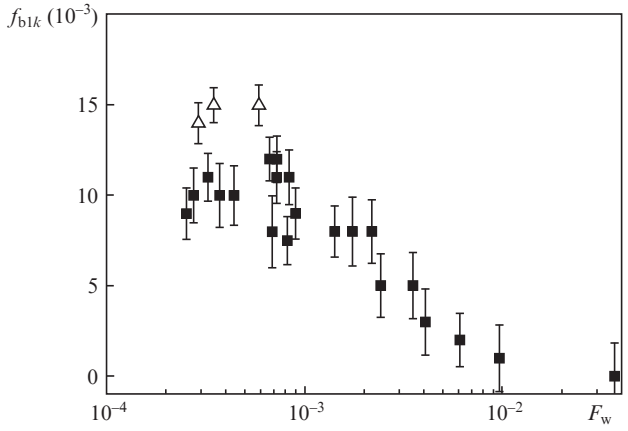

Figure 4. Dependence of the nonequilibrium content of vibrationally excited $O_2(b, v=1)$ molecules on the fraction of water vapor in the O_2(X)– O_2(a)–H_2O mixture at ODS heights of (■) 8 and (△) 15 mm.

At a water vapour content $F_w < 10^{-3}$ a number of experiments were performed with the optical window located 1.5, 6, and 8 cm below the WVT (along the flow). No rise in f_{b1k} with increasing distance from the WVT was found. An increase in

the distance from the WVT within 4–8 cm led to a change in the gas temperature from 370 to 350 K, and the concentration n_a changed within $(2.3–1.5)\times10^{17}$ cm^{-3}. At a distance of 1.5 cm from the WVT the gas temperature was 310 K. For the ODS with a channel height of 1.5 cm the f_{b1k} value generally reached 1.2×10^{-2}. Some experiments (Fig. 4) yielded $f_{b1k} \approx 1.5\times10^{-2}$.

4. Analysis and discussion

Let us relate the number of vibrational quanta generated in reactions (1) and (2) to the found nonequilibrium $O_2(b,v=1)$ content. The prodiction of vibrationally excited O_2 and H_2O molecules is followed by fast resonant EE and VV exchanges between oxygen molecules:

$$O_2(b,v=1) + O_2(X,v=0) \leftrightarrows O_2(X,v=1) + O_2(b,v=0), \quad (6)$$

$$O_2(b,v=1) + O_2(a,v=0) \leftrightarrows O_2(a,v=1) + O_2(b,v=0), \quad (7)$$

$$O_2(a,v=1) + O_2(X,v=0) \leftrightarrows O_2(X,v=1) + O_2(a,v=0), \quad (8)$$

$$O_2(X,v=2) + O_2(X,v=0) \leftrightarrows O_2(X,v=1) + O_2(X,v=1), \quad (9)$$

VV exchange with water molecules,

$$H_2O(1) + O_2(0) \rightarrow H_2O(0) + O_2(1) \quad (10)$$

and vibrational relaxation

$$O_2(1) + M \rightarrow O_2(0) + M, \quad (11)$$

$$O_2(1) + \text{wall} \rightarrow O_2(0) + \text{wall}, \quad (12)$$

$$H_2O(1) + M \rightarrow H_2O(0) + M, \quad (13)$$

$$H_2O(1) + \text{wall} \rightarrow H_2O(0) + \text{wall}. \quad (14)$$

Here, $H_2O(1) = H_2O(010)$; $H_2O(0) = H_2O(000)$, and $O_2(0)$ and $O_2(1)$ are oxygen molecules with $v=0$ and $v=1$, respectively, in any electronic state. The rate constants of direct reactions (in cm^3 s^{-1}) are as follows: $k_6 = 1.5\times10^{-11}$ [21], $k_8 = 5.6\times10^{-11}$ [1], $k_9 = 2\times10^{-13}$ [9], $k_{11}^{O_2}(M = O_2, T = 370\ K) = 10^{-17}$, $k_{11}^{w}(M = H_2O) = 4\times10^{-15}$, $k_{13}^{w}(M = H_2O) = 5.1\times10^{-11}$, $k_{13}^{O_2}(M = O_2) = 4\times10^{-14}$ [10], $k_{10}^{X} = 6.6\times10^{-13}$ for $O_2(X)$ [10]. Since $O_2(X)$ and $O_2(a)$ molecules are characterised by similar energies of vibrational quanta, it is reasonable to assume that $k_{10}^{a} \approx k_{10}^{X}$ for $O_2(a)$ in reaction (10). The rate constants of the reverse reactions $k_{10r}^{X} = k_{10}^{X}\exp[(E_X - E_w)/T]$ and $k_{10r}^{a} = k_{10}^{a}\times\exp[(E_a - E_w)/T]$, where $E_w = 2295$ K, $E_X = 2239$ K, and $E_a = 2134$ K are the vibrational energies of $H_2O(1)$, $O_2(X,v=1)$, and $O_2(a,v=1)$ molecules, respectively. The rate constant $k_{11}^{O_2}$ is assumed to be the same for $O_2(X,v=1)$ and $O_2(a,v=1)$ molecules [22, 23].

As far as we know, the rate constant k_7 of reaction (7) has not been measured, but it is pertinent to equate it to 10^{-11} cm^3 s^{-1}, as for reactions (6) and (8). The rate constants of reverse reactions (6)–(8) are as follows: $k_{6r} = k_6\times\exp[(E_X - E_b)/T]$, $k_{7r} = k_7\exp[(E_a - E_b)/T]$, $k_{8r} = k_8\exp[(E_X - E_a)/T]$. Since the dependence of f_{b1k} on the degree of chlorine utilisation was not observed in these experiments, we can suggest that $k_{11}^{Cl_2}(M = Cl_2) \le k_{11}^{O_2}$.

The destruction rate of vibrationally excited molecules of the ith type, concentrated in a narrow layer between the ODS walls, on these walls can be estimated from the formula

$$K_{ci} = \left(\frac{h^2}{8D} + \frac{2h}{\bar{u}\gamma_i}\right)^{-1}, \quad (15)$$

where γ_i is the surface deexcitation coefficient, $\bar{u}$ is the average thermal velocity, D is the diffusion coefficient, and h is the ODS height. For the on-wall $H_2O(1)$ deexcitation probability $\gamma_w \sim 1$ the $H_2O(1)$ destruction rate is $K_{cw} \sim 10^2$ c^{-1}.

Let us find f_{b1k} at $F_w < 10^{-3}$. The rate of EE-exchange reactions (6)–(9) significantly exceed the rate of reactions (10)–(14), because under our experimental conditions $n_w \ll n_a, n_X$, $n_b \ll n_a, n_X$, $n_{b1} \ll n_{a1}, n_{X1}$, where n_{b1}, n_{a1}, n_{X1}, and n_X are $O_2(b,v=1)$, $O_2(a,v=1)$, $O_2(X,v=1)$, $O_2(X,v=0)$ concentrations, respectively. The possible formation of $O_2(v=2)$ in reactions (1) and (2) is accompanied by fast EE exchanges $O_2(b,v=2) + O_2(X,v=0) \rightarrow O_2(b,v=0) + O_2(X,v=2)$, $O_2(a,v=2) + O_2(X,v=0) \rightarrow O_2(a,v=0) + O_2(X,v=2)$ [1] and VV exchange (9). As a result most of generated vibrational quanta are accumulated in $O_2(a,v=1)$ and $O_2(X,v=1)$ molecules. The time scale on which reactions (6)–(8) occur is much smaller than 3×10^{-2} s – the time of gas flow passage by a distance of 4 cm from WVT to the spectrum measurement point. Under these conditions the following equations for the quasi-stationary relative contents $f_{a1} = n_{a1}/n_a$ and $f_{b1} = n_{b1}/n_b$ for $O_2(a,v=1)$ and $O_2(b,v=1)$ molecules were obtained in [24, 27]:

$$f_{a1} = c_a f_{1k} + f_{a1T},\ f_{b1} = c_b f_{1k} + \frac{p_{11}k_2F_w}{k_6(1-Y) + k_7Y} + f_{b1T}, \quad (16)$$

where p_{11} is the production probability of $O_2(b,v=1)$ in reaction (1); $f_{1k} \approx (n_{a1k} + n_{X1k})/n_{O_2}$ is the nonequilibrium part of the relative content of oxygen molecules in the vibrational state with $v = 1$; n_{a1k} and n_{X1k} are nonequilibrium concentrations of $O_2(a,v=1)$ and $O_2(X,v=1)$ molecules, respectively; $c_a = f_{a1T}[Yf_{a1T} + (1-Y)f_{X1T}]^{-1}$; $c_b = f_{b1T}[Yf_{a1T} + (1-Y)f_{X1T}]^{-1}$.

The values $f_{X1T} = \exp(-E_X/T)$ and $f_{a1T} = \exp(-E_a/T)$, as well as the previously found f_{b1T} value, determine the thermal equilibrium fraction of vibrationally excited molecules in the corresponding electronic state.

Let us determine the nonequilibrium part f_{1k} of the relative content of $O_2(a)$ and $O_2(X)$ molecules in the vibrational state with $v = 1$ at $F_w < 10^{-3}$. As was shown above, f_{b1k} does not increase when the gas flow passes a distance of 4–8 cm from the WVT. Therefore, both the f_{1k} and f_{b1k} values are quasi-stationary along the flow and determined by the balance between the pumping and vibrational energy relaxation. Reactions (1) and (2) produce vibrational quanta of O_2 molecules at the rate $k_1n_a^2q_1 + k_2n_wn_bq_2 = k_1n_a^2(q_1 + q_2)$ and vibrational quanta of H_2O molecules at the rate $k_2n_wn_bm_2 = k_1n_a^2m_2$, because $n_b = (k_1/k_2)n_a^2/n_w$. Here, q_1 and q_2 are the average numbers of vibrational oxygen quanta, generated in reactions (1) and (2), and m_2 is the average number of 'bending' vibrational quanta of water molecules, generated in reaction (2). Under the experimental conditions $k_{10}n_{O_2} \gg K_{cw} + k_{13}^{w}n_w + k_{13}^{O_2}n_{O_2}$; hence, $H_2O(1)$ molecules supply vibrational quanta mainly to the $O_2(1)$ reservoir rather than to the thermal reservoir, and the total production rate of vibrational oxygen quanta is $k_1n_a^2(q_1 + q_2 + m_2)$. The relaxation rate of the nonequilibrium part of vibrational energy, which is independent of the water concentration, is $f_{1k}n_{O_2}(K_{cO_2} + k_{11}^{O_2}n_{O_2})$, where K_{cO_2} is the rate constant of $O_2(1)$ vibrational relaxation on walls in pro-

cess (12). The balance of the production and annihilation rates of vibrational quanta $k_1 n_a^2(q_1 + q_2 + m_2) = f_{1k} n_{O_2}(K_{cO_2} + k_{12}^{O_2} n_{O_2})$ yields the following expression for the nonequilibrium part of relative $O_2(b, v=1)$ content:

$$f_{b1k} = \frac{c_b}{n_{O_2}} \frac{(q_1 + q_2 + m_2) k_1 n_a^2}{K_{cO_2} + k_{11}^{O_2} n_{O_2}} + \frac{p_{11} k_2 F_w}{k_6(1 - Y) + k_7 Y}. \quad (17)$$

When estimating the sum $q_1 + q_2 + m_2$ the second term in (17) can be neglected, because it is smaller than 10^{-3}, while $f_{b1k} \geq 10^{-2}$ at $F_w < 10^{-3}$. According to [15, 25], $k_1 = (3.5 \pm 0.5) \times 10^{-17}$ cm^3 s^{-1} at $T = 370$ K. Unfortunately, we could not find any published data on the $O_2(1)$ deexcitation probability γ_{O_2} in reaction (12). To evaluate γ_{O_2} and K_{cO_2}, we use the fact that in the above-described experiments the maximum increase in f_{b1k} with an increase in the ODS height from 0.8 to 1.5 cm was a factor of 1.5. Using Eqns (15) and (17), we obtain the estimate $\gamma_{O_2} \approx (0.4–1.5) \times 10^{-3}$. This value is close to the relaxation coefficient of $N_2(v=1)$ molecules on nonmetallic surfaces [26]. At $T = 370$ K, pressure of 26 Torr, and $h = 0.8$ cm, we have $c_b = 1.61$ and the relaxation rate $K_{cO_2} + k_{11}^{O_2} n_{O_2} \approx 18–30$ s^{-1}. Substitution of $f_{b1k} \approx 10^{-2}$ and $n_a = 2.3 \times 10^{17}$ cm^{-3} into Eqn (17) yields $k_1 n_a^2(q_1 + q_2 + m_2) \approx 10^{17}$ cm^{-3} s^{-1} and $q_1 + q_2 + m_2 = 0.05 \pm 0.03$. The error ± 0.03 for $q_1 + q_2 + m_2$ is determined by the errors of the parameters k_1 (13%), n_a^2 (9.5%), f_{1k} (10%), and γ_{O_2}.

The maximum values $q_1 \approx 0.05$ and probabilities $p_{11} = q_1 \approx 0.05$, and $p_{12} = q_1/2 \approx 0.025$ of production of $O_2(b, v=1)$ or $O_2(b, v=2)$, respectively, in reaction (1) were obtained on the assumption that $q_2 = m_2 = 0$ and a zero contribution from other potential sources of $O_2(v>0)$ and $H_2O(v>0)$ molecules. For example, if deexcitation $O_2(a) + M \rightarrow O_2(X, v>0) + M$ occurs, the parameter q_1, according to the estimation, should be even smaller. The value $p_{11} = 0.05$ is in agreement with the result of [6]. The obtained estimate of probability $p_{12} = 0.025$ is much smaller than that reported in [3]: 0.64. Note that the probability $p_{12} \approx 0.64$ was obtained in [3] by comparing the emission intensities of $O_2(b)$ molecules from the first three vibrational levels in post-discharge O_2 flow. As was noted in [21], the high content of $O_2(b, v=2)$ molecules, observed in [3] in post-discharge O_2 flow, is most likely to be caused by the secondary processes with participation of atomic oxygen.

COILs are most often based on SOGs generating O_2–$O_2(a)$–H_2O gas at a temperature $T > 320$ K and relative concentrations $F_w > 3 \times 10^{-2}$ and $Y \approx 0.6$ [8]. In this case, $[Yk_{10r}^a + (1 - Y)k_{10r}^X] n_w \gg (k_{11}^{O_2} n_{O_2} + k_{11}^w n_w + K_{cO_2})$ and $(k_{13}^{O_2} n_{O_2} + k_{13}^w k n_w + K_{cw}) > [Yk_{10}^a + (1 - Y)k_{10}^X] n_{O_2}$; i.e., $O_2(1)$ molecules dissipate mainly through the energy transfer to $H_2O(0)$ molecules in reaction (10) with subsequent $H_2O(1)$ relaxation. The balance between pumping and vibrational energy relaxation for oxygen molecules, $[Yk_{10r}^a + (1 - Y)k_{10r}^X] n_w (f_{1k} n_{O_2}) \approx k_1 n_a^2 (q_1 + q_2)$, yields [27]

$$f_{1k} = \frac{(q_1 + q_2) k_1 Y^2}{[Yk_{10r}^a + (1 - Y)k_{10r}^X] F_w}. \quad (18)$$

After substituting $q_1 + q_2 \leq 0.08$, $F_w > 3 \times 10^{-2}$, $k_1 \approx 3.5 \times 10^{-17}$ cm^3 s^{-1}, $k_{10r}^a \approx k_{10r}^X \approx 5 \times 10^{-13}$ cm^3 s^{-1}, and $Y = 0.6$ into Eqn (18), we obtain $f_{1k} < 10^{-4}$. The thermal equilibrium of $O_2(a, v=1)$ content at the SOG output exceeds 10^{-3}, whereas its nonequilibrium part $f_{a1k} = c_a f_{1k} < 10^{-4}$ at $T > 320$ K. According to [27], at $p_{12} = 0.025$ the nonequilibrium $O_2(a, v=2)$ content with respect to $O_2(a, v=0)$ is 10^{-7}, whereas the thermal equilibrium $O_2(a, v=2)$ content exceeds 10^{-6} at $T > 320$ K. Therefore, at the output of SOGs that are used in COILs, the vibrational populations of both $O_2(a, v=1)$ and $O_2(a, v=2)$ are very close to the thermal equilibrium value. In [5, 28], the $O_2(a, v=1)$ content in the $O_2(X)$–$O_2(a)$–H_2O gas flow at a high pressure of $O_2(a)$ (few tens of Torr) was $\sim 10^{-2}$. Such a high $O_2(a, v=1)$ content is likely to be caused by the high gas temperature (above 450 K) at the SOG output as a result of the heat release in reaction (1) at a high $O_2(a)$ pressure [29].

5. Conclusions

The measurements of the absolute spectral irradiance in the range of 600–800 nm in the O_2–$O_2(a)$– H_2O gas mixture produced by a chemical singlet-oxygen generator made it possible to determine the concentration of electronic-excited particles. Nonequilibrium population of the first vibrational level of $O_2(b)$ molecules was clearly observed. Under our experimental conditions, the nonequilibrium $O_2(b, v=1)$ content ($\sim 10^{-2}$) was found to be independent of the concentration of water vapour when its relative content did not exceed 10^{-3}. The analysis of the results obtained, using the data on the kinetic processes in the O_2–$O_2(a)$–H_2O mixture, showed the maximum average number of vibrational quanta generated in reaction (1) is 0.05 ± 0.03. This value is in agreement with the earlier result of [6]. The predicted content of $O_2(a, v=1)$ and $O_2(a, v=2)$ in the gas mixture at the output of SOGs that is most often used in chemical oxygen–iodine lasers corresponds to a greater extent to thermal equilibrium. Nevertheless, this conclusion does not exclude the potentially important role of $O_2(a, v=1)$ and $O_2(a, v=2)$ molecules in the mechanism of molecular iodine dissociation in the active medium of oxygen–iodine laser.

Acknowledgements. I am grateful to A.N. Khvatov for his help at carrying out the experiments and to V.N. Azyazov and P.A. Mikheev for helpful discussions.

References

1. Slanger T.M., Copeland R.A. *Chem. Rev.*, **103**, 4731 (2003).
2. Yanovskii V.Ya. *Khim. Fiz.*, **10**, 291 (1991).
3. Schurath U. *J. Photochem.*, **4**, 215 (1975).
4. Biryukov A.S., Shcheglov V.A. *Kvantovaya Elektron.*, **13**, 510 (1986) [*Sov. J. Quantum Electron.*, **16**, 333 (1986)].
5. Browne R.J., Ogryzlo E.A. *Proc. Chem. Soc.*, **117**, 89 (1964).
6. Derwent R.G., Thrush B.A. *Trans. Faraday Soc.*, **67**, 2036 (1971).
7. Ogryzlo E.A., Thrush B.A. *Chem. Phys. Lett.*, **24**, 314 (1974).
8. Waichman K., Rybalkin V., Katz A., et al. *J. Appl. Phys.*, **102**, 013108 (2007).
9. Kalogerakis K.S., Copeland R.A., Slanger T.G. *J. Chem. Phys.*, **123**, 044309 (2005).
10. Huestis D.L. *J. Phys. Chem. A.*, **110**, 6638 (2006).
11. Azyazov V.N., Zagidullin M.V., Nikolaev V.D., Svistun M.I., Khvatov N.A. *Kvantovaya Elektron.*, **22**, 443 (1995) [*Quantum Electron.*, **25**, 423 (1995)].
12. Naus H., Ubachs W. *Appl. Opt.*, **38**, 3423 (1999).
13. Borrel P., Rich N.H. *Chem. Phys. Lett.*, **99**, 144 (1983).
14. Cheah S., Lee Y., Ogilvie J.F. *J. Quantum Spectr. Rad. Transfer*, **64**, 467 (2000).
15. Lilenfeld H.V., Carr P.A.G., Hovis F.E. *J. Chem. Phys.*, **81**, 5730 (1984).
16. Aviles R.G., Muller D.F., Houston P.L. *Appl. Phys. Lett.*, **37**, 358 (1980).
17. Rothman L.S., Jacquemart D., Barbe A., et al. *J. Quantum Spectr. Rad. Transfer*, **96**, 139 (2005).
18. Krupenie P.H. *J. Phys. Chem. Ref. Data*, **1**, 423 (1972).
19. Knickelbein M.B., Marsh K.L., Sercel J., Siebert L.D., Busch G.E. *IEEE J. Quantum Electron.*, **24**, 1278 (1988).

20. Choo K.Y., Leu M. *Int. J. Chem. Kinet*., **17**, 1155 (1985).
21. Bloemink H.I., Copeland R.A., Slanger T.G. *J. Chem. Phys.*, **109**, 4237 (1998).
22. Borrell P.M., Borrell P., Grant K.R. *J. Chem. Soc. Faraday Trans.*, **76**, 923 (1980).
23. Parker J.G., Ritke D.N. *J. Chem. Phys.*, **59**, 3713 (1973).
24. Antonov I.O., Azyazov V.N., Ufimzev N.I. *J. Chem. Phys*., **119**, 10638 (2003).
25. Heidner R.F., Gardner C.E., El-Sayed T.M., Segal G.I., Kasper J.V.V. *J. Chem. Phys.*, **74**, 5618 (1981).
26. Black G., Wise H., Schechter S., Sharpless R.L. *J. Chem. Phys*., **60**, 3526 (1974).
27. Azyazov V.N., Pichugin S.Yu., Safonov V.S., Ufimtsev N.I. *Kvantovaya Elektron.*, **31**, 794 (2001) [*Quantum Electron*., **31**, 794 (2001)].
28. Azyazov V.N., Nikolaev V.D., Svistun M.I., Ufimtsev N.I. *Kvantovaya Elektron.*, **29**, 767 (1999) [*Quantum Electron*., **32**, 747 (1999).
29. Watanabe G., Sugimoto D., Tei K., Fujioka T. *IEEE J. Quantum Electron.*, **40**, 1030 (2004).